Mapping of contributions from car-exterior aerodynamic sources to an in-cabin reference signal using Clean-SC

Jørgen HALD[1]; Hiroshi KURODA[2]; Takafumi MAKIHARA[3]; Yutaka ISHII[4]

[1] Brüel & Kjær SVM A/S, Denmark

[2,3] Toyota Motor Corporation, Japan

[4] Brüel & Kjaer Japan, Japan

ABSTRACT

Use of an out-of-flow array in a wind tunnel to map car-exterior aerodynamic noise sources will typically show the contributions to the sound pressure at the array. The cross-spectral matrix is first averaged, followed by beamforming and use of a deconvolution technique, such as Clean-SC, to improve spatial resolution and to suppress sidelobes. Clean-SC makes use of the fact that the aerodynamic noise sources across the exterior car surface are highly incoherent, so it builds up a sparse distribution of incoherent point sources on the mapping surface, which together represent the measured cross-spectral matrix to a chosen accuracy. The main idea of the present paper is to produce a Clean-SC map, where each point source is assigned a strength equal to that part of a measured in-cabin reference signal, which is coherent with the point source. Effectively, a map is obtained of the car-exterior contributions to the in-cabin reference. A validation is performed first based on measurements on loudspeakers around a car, in which case the correct contributions from individual speakers can be easily measured. Next, an application to real aerodynamic noise sources around a car in a wind tunnel is described and discussed.

Keywords: Wind noise, in-cabin contribution, beamforming.
I-INCE Classification of Subjects Number(s): 74.7, 74.1

1. INTRODUCTION

When an out-of-flow array is used for locating and quantifying aerodynamic noise sources on a car in a wind tunnel, the obtained maps will show contributions to the sound pressure measured at the array. Usually, however, localization and quantification of sources to the flow noise experienced at the driver and passenger positions in the cabin are of much higher interest. The work described in the present paper relates to that issue.

One possibility is to use a reference microphone at a listener's position in the cabin and apply typically Delay And Sum (DAS) beamforming to that part of the measured sound, which is coherent with the reference signal. However, the output will not provide a direct quantification of the contributions at the reference. Also, because the processed sound field is coherent (with the reference signal), it is not suited for use with standard deconvolution methods, such as Non-Negative Least Squares (NNLS) (1) and Clean-SC (2), which use a source model of incoherent point sources.

The method of the present paper aims directly at estimating the contributions to a reference signal from different incoherent sources on the exterior of a car body. The method is integrated with the iterative Clean-SC algorithm, which uses as input an averaged cross-power spectral matrix (CSM) measured with the array. In each iteration, a DAS beamforming is performed, a point source is located at the peak, and all components of the CSM coherent with the peak signal are removed. According to the extension described in the present paper, the part of the reference signal coherent with the peak is also calculated in each iteration.

Section 2 describes the theory, first for the standard Clean-SC algorithm, and then for the extension

[1] jorgen.hald@bksv.com
[2] hiroshi_kuroda@mail.toyota.co.jp
[3] takafumi_makihara@mail.toyota.co.jp
[4] yutaka.ishii@bksv.com

to obtain the coherent auto-power components of a measured reference signal. Results from practical measurements are presented in Section 3, focusing on validation of the new method. In Section 3.1, a validation based on loudspeaker sources is described, while Section 3.2 presents and discusses the application to aerodynamic sources around a vehicle. Finally, Section 4 contains a summary.

2. THEORY

2.1 Clean-SC deconvolution

The Clean-SC deconvolution method for beamforming was introduced by Sijtsma (2). To facilitate the description of the extension to be introduced in the following section, the theory of the basic method will be outlines here.

Consider an array measurement for which the MxM complex Hermitian matrix $\mathbf{C}$ of cross-power spectra has been averaged, M being the number of microphones. We consider focusing of the array at a set of J positions indexed by $j = 1, 2, \ldots, J$. The focused pressure auto-power B_{jj} at position j is calculated by Delay And Sum (DAS) beamforming using the steering vector $\mathbf{w}_j$:

$$B_{jj} = \mathbf{w}_j^H \mathbf{C} \mathbf{w}_j , \tag{1}$$

where H represents Hermitian (conjugate) transposed. A DAS map is calculated this way at each iteration number k of the Clean-SC algorithm, but using a so-called Degraded cross-spectral matrix $\mathbf{C}^{(k)}$, where the components coherent with all previously identified sources have been subtracted. The iteration is stated with the full matrix:

$$\mathbf{C}^{(0)} \equiv \mathbf{C} . \tag{2}$$

Thus, at iteration k the DAS map is calculated using the degraded cross-spectral matrix:

$$B_{jj}^{(k)} = \mathbf{w}_j^H \mathbf{C}^{(k-1)} \mathbf{w}_j . \tag{3}$$

The cross spectrum between the focused signals at focus points j and i can be shown to be:

$$B_{ij}^{(k)} = \mathbf{w}_i^H \mathbf{C}^{(k-1)} \mathbf{w}_j . \tag{4}$$

Assume now that the peak of the DAS map calculated at iteration k is at focus point number κ. The peak of the DAS map is then:

$$B_{\max}^{(k)} \equiv B_{\kappa\kappa}^{(k)} = \mathbf{w}_\kappa^H \mathbf{C}^{(k-1)} \mathbf{w}_\kappa . \tag{5}$$

We assign a point source to that position with amplitude to be considered subsequently, and we subtract from the cross-spectral matrix all signal components coherent with the focused signal at the DAS peak. The fact that we subtract a single coherent component implies that its contribution to the cross-spectral matrix has rank equal to one. The subtraction can therefore in general be expressed as follows:

$$\mathbf{C}^{(k)} = \mathbf{C}^{(k-1)} - \mathbf{p}^{(k)} \mathbf{p}^{(k)H} . \tag{6}$$

Since the subtraction removes everything coherent with the DAS peak at position κ, the vector $\mathbf{p}^{(k)}$ must be derived from the requirement that DAS beamforming based on $\mathbf{C}^{(k)}$ must predict the cross spectra between point κ and all other points to equal zero:

$$B_{j\kappa}^{(k+1)} = \mathbf{w}_j^H \mathbf{C}^{(k)} \mathbf{w}_\kappa = \mathbf{w}_j^H \left[\mathbf{C}^{(k-1)} - \mathbf{p}^{(k)} \mathbf{p}^{(k)H} \right] \mathbf{w}_\kappa = 0, \quad j = 1,2,\ldots J . \tag{7}$$

This requirement will of course be fulfilled if:

$$\left[\mathbf{C}^{(k-1)} - \mathbf{p}^{(k)} \mathbf{p}^{(k)H} \right] \mathbf{w}_\kappa = 0 , \tag{8}$$

or equivalently:

$$\mathbf{C}^{(k-1)} \mathbf{w}_\kappa = \mathbf{p}^{(k)} \mathbf{p}^{(k)H} \mathbf{w}_\kappa . \tag{9}$$

Assuming a solution of the form:

$$\mathbf{p}^{(k)} = \alpha \mathbf{C}^{(k-1)} \mathbf{w}_\kappa , \tag{10}$$

containing an unknown scaling factor α, and inserting that assumed solution in Eq. (9), we get by application of Eq. (5) and the fact that the cross-spectral matrix is Hermitian:

$$\mathbf{C}^{(k-1)} \mathbf{w}_\kappa = \mathbf{p}^{(k)} \mathbf{p}^{(k)H} \mathbf{w}_\kappa = \alpha^2 B_{\kappa\kappa}^{(k)} \mathbf{C}^{(k-1)} \mathbf{w}_\kappa . \tag{11}$$

Clearly, Eq. (11) is fulfilled if:

$$\alpha = 1 \Big/ \sqrt{B_{\kappa\kappa}^{(k)}} , \tag{12}$$

which can be inserted in Eq. (10) to give:

$$\mathbf{p}^{(k)} = \frac{1}{\sqrt{B_{\kappa\kappa}^{(k)}}} \mathbf{C}^{(k-1)} \mathbf{w}_{\kappa} . \tag{13}$$

With $\mathbf{p}^{(k)}$ known, the reduced cross-spectral matrix $\mathbf{C}^{(k)}$ for the next iteration can be calculated using Eq. (6), a new DAS map can be calculated, the peak can be identified, the new vector $\mathbf{p}^{(k+1)}$ can be calculated etc. The iteration is typically stopped, when the peak in the DAS map has been reduced by some specified factor, for example by 12 decibel. Assuming that this happens after K iterations, then because of Eqs. (2) and (6):

$$\mathbf{C} = \sum_{k=1}^{K} \mathbf{p}^{(k)} \mathbf{p}^{(k)H} + \mathbf{C}^{(K)} . \tag{14}$$

The coherent sound field identified in each iteration can be visualized as a point source or a smeared point source at the peak of the DAS map from that iteration. The diagonal of the cross-spectral matrix $\mathbf{C}$ contains the microphone pressure auto-power spectra. Thus, by application of Eq. (14) we get the following expression for the average pressure auto-power P_{avg} over all array microphones:

$$P_{\text{avg}} \equiv \frac{1}{M} \sum_{m=1}^{M} C_{mm} = \frac{1}{M} \sum_{k=1}^{K} \left\| \mathbf{p}^{(k)} \right\|_2^2 + \frac{1}{M} \sum_{m=1}^{M} C_{mm}^{(K)} . \tag{15}$$

Clearly, the contribution $P_{\text{avg}}^{(k)}$ from partial source number k is:

$$P_{avg}^{(k)} = \frac{1}{M} \left\| \mathbf{p}^{(k)} \right\|_2^2 \tag{16}$$

This pressure auto-power contribution will typically be the amplitude of partial source number k shown in a map. In order to obtain smooth maps, a smoothing function is applied that distributes the power of each point source over some small area, see reference (2), where also the use of a "loop gain" factor to stabilize the iteration is described.

The Clean-SC method as published by Sijtsma (2) includes an iterative Diagonal Removal (DR) algorithm, avoiding use of the measured auto-power spectra from the array, since these may be contaminated by severe flow noise. In the present work, we found that DR algorithm to work well for identification of the stronger sources, but to fail for the weaker sources. A new algorithm was therefore applied, which solves a so-called Semi-definite Program, minimizing the sum of the auto-power elements on the diagonal of the cross-spectral matrix, while maintaining it positive semi-definite. The new algorithm, which is treated in more detail in a separate paper by Hald (3), is used in a pre-processing step, before application of the Clean-SC algorithm described above.

2.2 Clean-SC source contributions to a measured reference signal

We now consider the case, where beyond the array signals we measure also a reference signal. In a wind-tunnel application, typically the array will be out-of-flow, while a reference microphone will be in the cabin of a vehicle. Beyond the matrix $\mathbf{C}$ of cross-power spectra between the array microphones, we then measure also the vector $\mathbf{C}_{ra}$ of cross-power spectra between the reference signal and the array microphone signals. The goal is to extend the iteration of the previous section to provide the part of the reference auto-power spectrum coherent with each one of the identified incoherent point sources. Initially, we consider only the first step of the iteration, and subsequently the full iterative process is derived.

For the derivation, we need the cross-power spectrum C_{rb} between the reference and the beamformed signal at the DAS peak. The vector $\mathbf{C}_{ra}$ of reference-to-array cross spectra is obtained by FFT and averaging as described by the formula:

$$\mathbf{C}_{ra} = \overline{\mathbf{p} r^*} , \tag{17}$$

where r is the complex reference signal from an FFT, $\mathbf{p}$ is a corresponding vector of complex array microphone signals, * represents complex conjugate, and the bar on top represents averaging over FFT blocks (records). For the single FFT record, the beamformed signal b at the peak is the result of a focusing that uses the steering vector $\mathbf{w}$:

$$b = \mathbf{w}^H \mathbf{p} . \tag{18}$$

Notice that averaging of bb^* over FFT records leads to an expression of the form (1) for the beamformed auto-power signal C_{bb} at the DAS peak: $C_{bb} = \overline{bb^*} = \mathbf{w}^H \overline{\mathbf{p}\mathbf{p}^H} \mathbf{w} = \mathbf{w}^H \mathbf{C} \mathbf{w}$. The following expression for C_{rb}:

$$C_{rb} = \overline{br^*} = \overline{\mathbf{w}^H \mathbf{p} r^*} = \mathbf{w}^H \overline{\mathbf{p} r^*} = \mathbf{w}^H \mathbf{C}_{ra}, \tag{19}$$

now follows from Eqs. (17) and (18). In Eq. (19), the steering vector **w** performs a focusing operation across the array-microphone dimension in $\mathbf{C}_{ra}$, which is valid as well for the degraded matrices occurring during the below iteration. Finally, an expression for that part R of the reference auto-power spectrum, which is coherent with the beamformed signal at the DAS peak, can be obtained by application of a standard formula for Coherent Output Power, see for example reference (4):

$$R = \frac{|C_{rb}|^2}{C_{bb}} = \frac{\left|\mathbf{w}^H \mathbf{C}_{ra}\right|^2}{\mathbf{w}^H \mathbf{C} \mathbf{w}}. \tag{20}$$

In each iteration of the Clean-SC algorithm described in Section 2.1, the cross-power matrix **C** is degraded by subtracting all components coherent with the DAS peak before a new DAS beamforming is performed to identify the next independent source. To calculate in each iteration also the contribution R from the identified source to the measured reference signal, we need to degrade in the same way the reference-to-array cross-power vector $\mathbf{C}_{ra}$ by subtracting all components coherent with the DAS peak.

At iteration k we have the vector $\mathbf{C}_{ra}^{(k-1)}$ with the contributions from the first k-1 sources subtracted. Subtraction of a coherent contribution must be a rank-one update of the form:

$$\mathbf{C}_{ra}^{(k)} = \mathbf{C}_{ra}^{(k-1)} - \mathbf{p}^{(k)} r^{(k)*}, \tag{21}$$

where $\mathbf{p}^{(k)}$ is the vector of array-microphone pressure values (13) coherent with the DAS peak, and $r^{(k)}$ is the coherent part of the reference signal. We already know the auto-power of $r^{(k)}$ from the expression (20). The full expression can be obtained by requiring (similar as in the degradation of **C**) that the degraded vector $\mathbf{C}_{ra}^{(k)}$ implies the degraded cross spectrum $C_{r\kappa}^{(k)}$ between the reference and DAS peak number κ to equal zero. Use of Eq. (19) allows this to be expressed as:

$$C_{r\kappa}^{(k)} = \mathbf{w}_\kappa^H \mathbf{C}_{ra}^{(k)} = \mathbf{w}_\kappa^H \left(\mathbf{C}_{ra}^{(k-1)} - \mathbf{p}^{(k)} r^{(k)*}\right) = 0, \tag{22}$$

which can be solved for $r^{(k)}$:

$$r^{(k)*} = \frac{\mathbf{w}_\kappa^H \mathbf{C}_{ra}^{(k-1)}}{\mathbf{w}_\kappa^H \mathbf{p}^{(k)}}. \tag{23}$$

Here, the denominator can be rewritten through application of Eqs. (13) and (5):

$$\mathbf{w}_\kappa^H \mathbf{p}^{(k)} = \frac{1}{\sqrt{B_{\kappa\kappa}^{(k)}}} \mathbf{w}_\kappa^H \mathbf{C}^{(k-1)} \mathbf{w}_\kappa = \sqrt{B_{\kappa\kappa}^{(k)}}, \tag{24}$$

so finally we get:

$$r^{(k)*} = \frac{\mathbf{w}_\kappa^H \mathbf{C}_{ra}^{(k-1)}}{\mathbf{w}_\kappa^H \mathbf{p}^{(k)}} = \frac{\mathbf{w}_\kappa^H \mathbf{C}_{ra}^{(k-1)}}{\sqrt{B_{\kappa\kappa}^{(k)}}}. \tag{25}$$

Notice that Eq. (25) specifies the same contributed auto-power at the reference as Eq. (20):

$$R^{(k)} = \left|r^{(k)}\right|^2. \tag{26}$$

Together with the initialization:

$$\mathbf{C}_{ra}^{(0)} = \mathbf{C}_{ra}, \tag{27}$$

where $\mathbf{C}_{ra}$ is the vector of measured reference-to-array cross spectra, Eqs. (25) and (21) support a full integration with the standard Clean-SC algorithm of Section 2.1 to estimate the reference auto-power components coherent with each one of the Clean-SC sources. Since all sources of the Clean-SC source model are mutually incoherent, the calculated coherent power values $R^{(k)}$ constitute the contributions from the individual sources.

The reference contributions can be visualized in a map simply by use of the reference contributions $R^{(k)}$ instead of the array contributions $P_{\text{avg}}^{(k)}$ as source strengths for the identified point sources.

The resolution of sources and their contributions based on coherence has some limitation, some of the important ones being:

1. Only incoherent sources can be resolved by the basic Clean-SC algorithm of Section 2.1.
2. The use of the vector $\mathbf{C}_{ra}$ of measured reference-to-array cross spectra in the estimation of

source contributions to a reference implies that coherence loss between the reference and the array due to typically turbulence will cause an under-estimation of the contributions.

3. For a vehicle in a wind tunnel, there will be a huge number of independent (incoherent) sources around the vehicle. With *M* array microphones, a maximum of *M* independent sources and their contributions can be resolved and fully represented. Also, only sources with a significant contribution at the array will be included. Some of the results to be presented in Section 3.2 show that measurement with a single out-of-flow array does not pick up all sources. As a result, the sum of the estimated contributions is smaller than the measured total reference auto-power. However, such under-estimation will always be an issue with beamforming based on a cross-spectral matrix measured with an out-of-flow array.

3. MEASUREMENTS

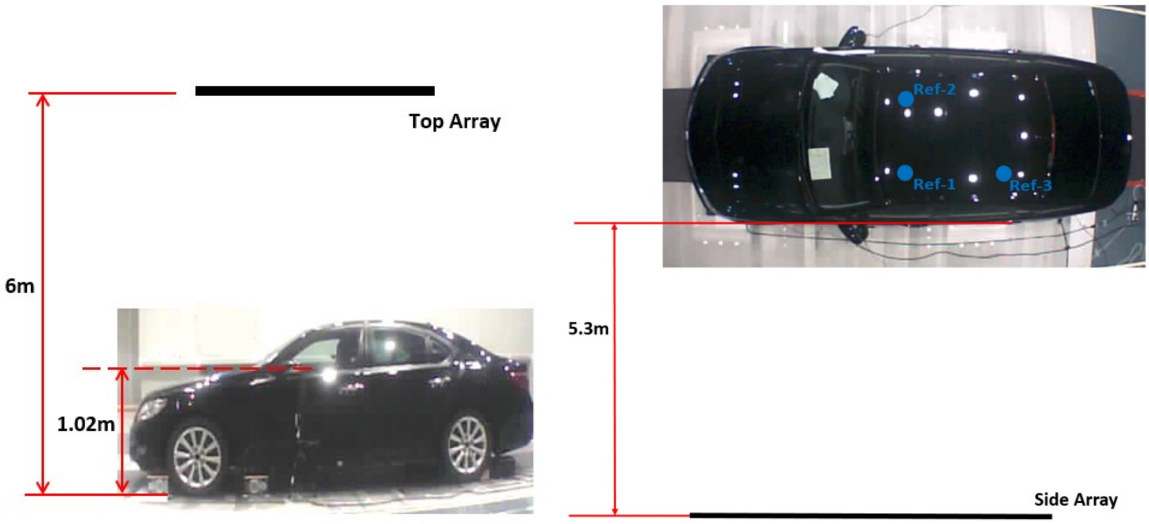

Figure 1 – Side view (left) and top view (right) of the measurement setup.

A series of measurements were taken in February 2015 on a Lexus LS 460 car in the semi-anechoic wind tunnel belonging to Toyota Motor Corporation. Data were recorded simultaneously by a 78-channel overhead array 6 m above the floor, by a 66-channel side array 5.3 m from the left side of the vehicle and by three references in the car cabin. The top array was a wheel with 3 m diameter, while the side array was a half wheel with 3.2 m diameter. Figure 1 illustrates the positions of the two arrays relative to the car, and the top view (right) indicates the positions of the reference microphones in the cabin (blue dots): Number 1 at the driver's head position, number 2 at the head position of the front-seat passenger, and number 3 at the left-side passenger position on the back seat.

A series of measurements were taken with no wind, but with a set of loudspeakers distributed around the car. For these measurements, which are dealt with in Section 3.1, the contribution from a selected loudspeaker could be measured directly by switching off the remaining speakers.

Another series of measurements were taken with no loudspeakers, but with a set of different wind speeds. In this case, an estimate of the contribution from the door mirrors was obtained by measuring with the mirrors on and off, and the contribution from the A-pillars could be estimated by measuring with and without a smoothing of these. The wind noise measurements are dealt with in Section 3.2.

3.1 Loudspeakers around the car, no wind

Five loudspeakers were positioned around the car as illustrated in Figure 2: Number 1 and 2 were placed behind the two door mirrors, while the remaining three were put on the floor to emulate wind noise sources around the wheels on the left side of the car, i.e. the same side as the side array. The speakers were excited by mutually incoherent pink noise signals, and the level of each one of the speakers 1, 3, 4 and 5 was adjusted initially to produce 70 dB overall sound pressure level at a center microphone of the side array. The excitation signal to speaker 2 was then set at same level as that supplied to speaker 1. Both speaker 1 and 2 were Brüel & Kjaer Omnisources Type 4295, so their radiated power should then be almost equal. The aim of the investigation was to determine the contribution from speaker 1 at the three reference microphones for a set of different levels of speaker

1: 70, 65 and 60 dB. The other four speakers were kept at their initial levels. To be able to check the estimation accuracy, each one of the three settings was measured a) with all speakers active, and, b) with all speakers except number 1 switched off. The most difficult case will probably be the estimation of the speaker 1 contribution at reference 2 with the speaker 1 excitation set at 60 dB.

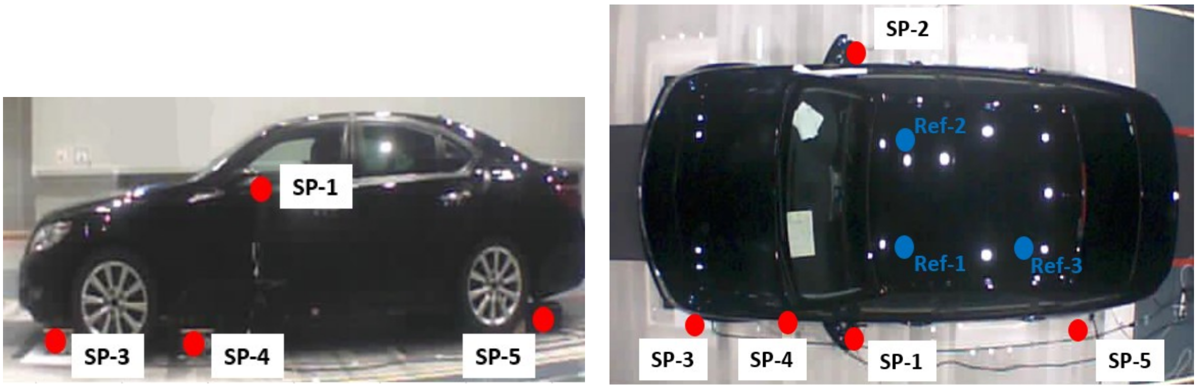

Figure 2 – Positions of the five loudspeakers around the car.

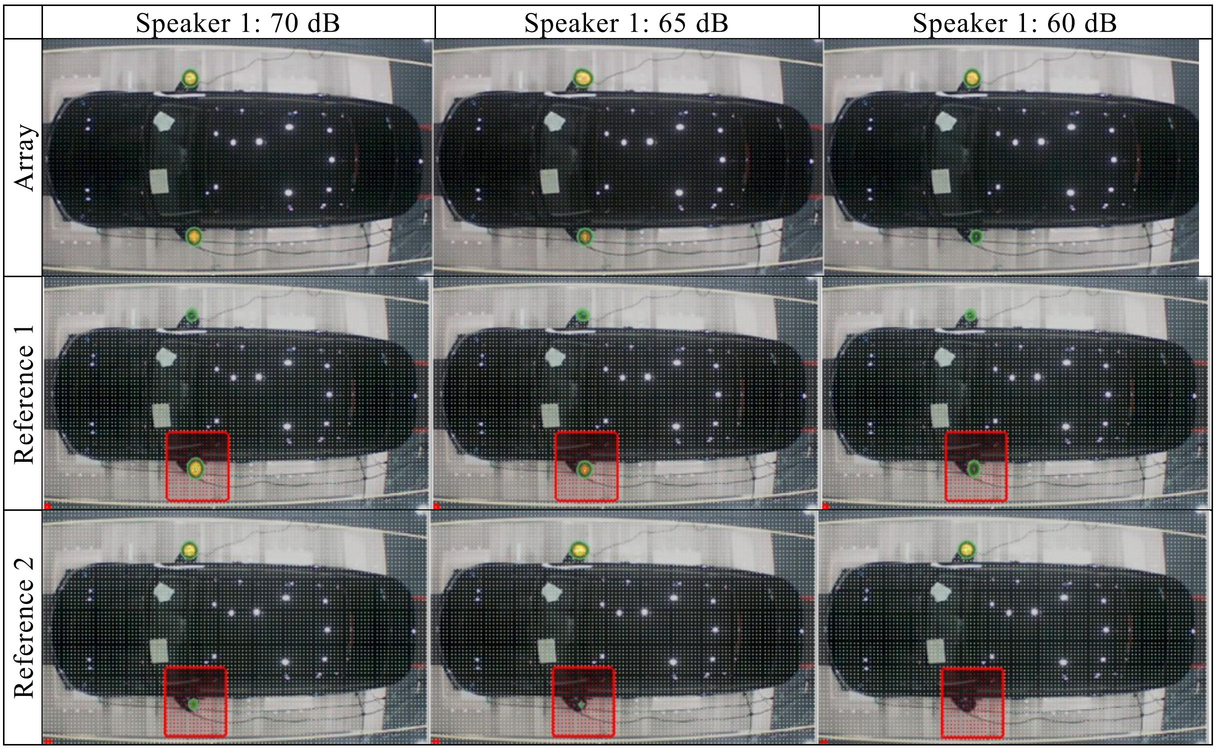

Figure 3 – Contour plots of contributions to array microphones (top row), to reference 1 (middle row) and reference 2 (bottom row) in the frequency interval 3-4 kHz. Display range is 25 dB, and for each row, the same scaling has been used.

Only results from the top array will be presented here. For each measurement, 10 seconds of time data were recorded, providing 319 averages with an 800-line FFT. The stopping criterion for the Clean-SC iteration was in all cases a 15 dB reduction of the peak level in the DAS map. Figure 3 contains contour plots of the contributions to the array microphones (top row, Eq. (16)), to reference 1 (middle row, Eq. (26)) and to reference 2 (bottom row, Eq. (26)) for the three different excitation levels of speaker 1 and covering the frequency range 3-4 kHz. The red rectangle shown in the two lower rows has been used for area-integration of the contributions from speaker 1, which will be presented subsequently. Notice that only contributions from speakers 1 and 2 are visible within the display range. The reasons are probably the sideward directivity of the three speakers on the floor and the fact that focusing is at the altitude of source 1 and 2 above ground, not on the floor.

From the top row of Figure 1, the following can be seen: With the initial 70 dB setting of all speakers, including speaker 1 (left plot), speaker 1 and 2 have almost equal average sound-pressure contributions to the array microphones. The two plots further right show the decreasing contribution from speaker 1, when its excitation is reduced. Looking at the maps of reference 1 contributions in the middle row, a very similar picture is seen with a constant, but now weaker contribution from speaker 2. This is due to reference 1 being much closer to speaker 1 than to speaker 2. After a 10 dB reduction of the speaker-1 excitation, speaker 1 and 2 have almost equal contributions at reference 1. For the contributions at reference-2, shown in the bottom row, speaker 2 is dominating already with equal excitations because of the propagation path differences, and with decreasing excitation of speaker 1, the difference between the contributions becomes very large.

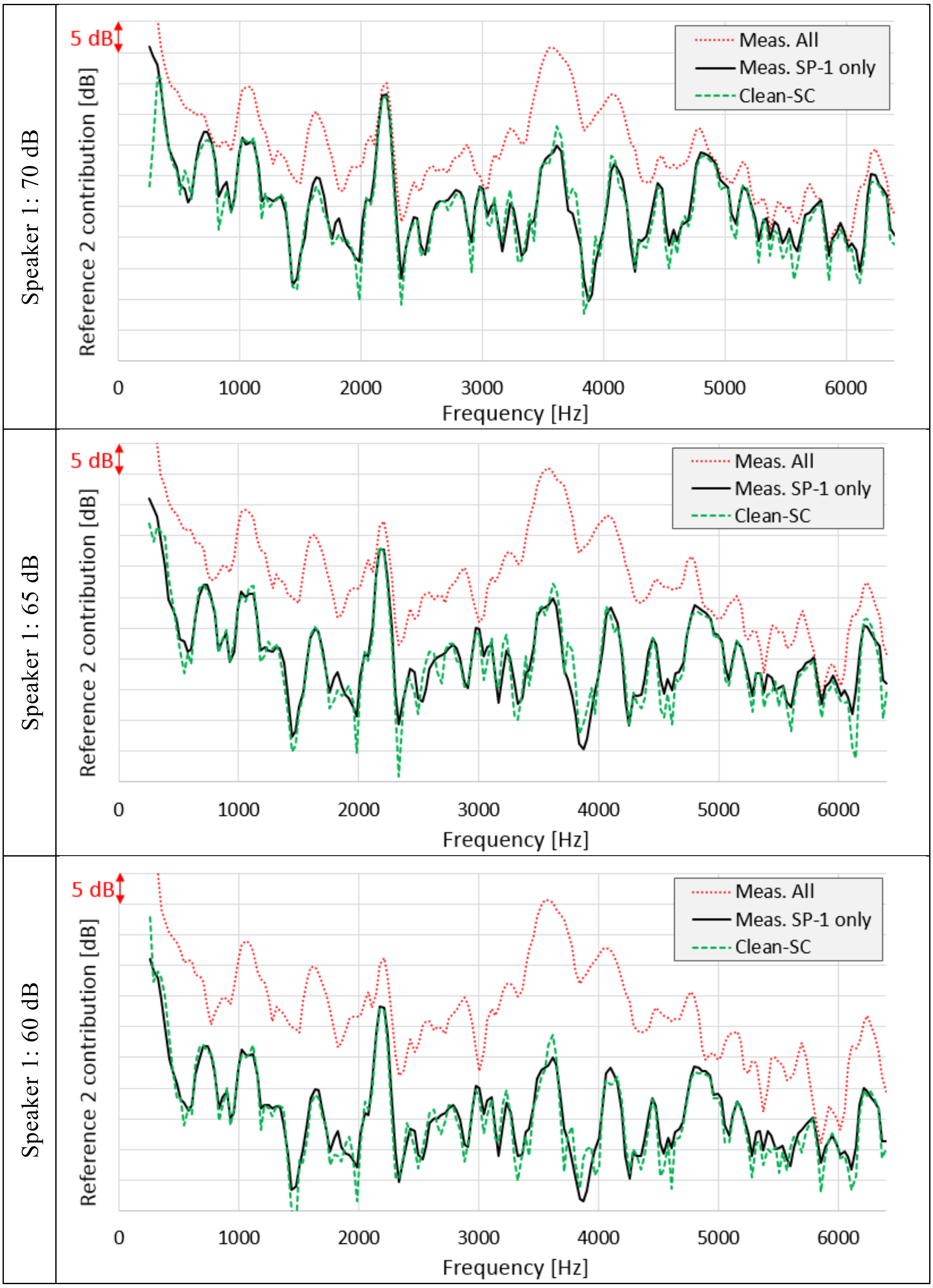

Figure 4 – Estimated speaker 1 contributions at reference 2 with three different settings of speaker 1 level.

Figure 4 contains spectra to illustrate the accuracy in the estimation of speaker 1 contributions at reference 2. The estimated spectra were obtained by area-integration of contour maps as those in the bottom row of Figure 3 across the red rectangle. The estimated contributions (dashed green) are compared with:

1. The measured sound pressure level at reference 2 with all speakers active (dotted red)
2. The measured sound pressure level at reference 2 with only speaker 1 active (solid black).

Ideally, the estimated contributions (dashed green) should equal the measured spectra with only speaker 1 active (solid black). Notice, however, that these two spectra are not measured simultaneously, which will always introduce small deviations.

For the case of speaker 1 at 70 dB (top plot in Figure 4), speakers 1 and 2 had approximately equal contributions at the array. The top, left contour plot in Figure 3 confirms this. Speaker 1 will therefore be accurately identified by Clean-SC. The estimation of the speaker 1 contribution at reference 2, however, involves the extraction of a weak component from a high-level incoherent speaker 2 contribution. With weaker excitation of speaker 1 (middle and bottom of Figure 4) the speaker 1 source strength estimation by Clean-SC becomes more challenging (see the top right contour plot in Figure 3), and based on that a weak coherent component in the reference 2 signal must be extracted. The results in Figure 4 show that accurate reference contribution estimates can be obtained under these conditions, with contributions 20 dB lower than the total measured reference signal.

3.2 Wind at 120 km/h

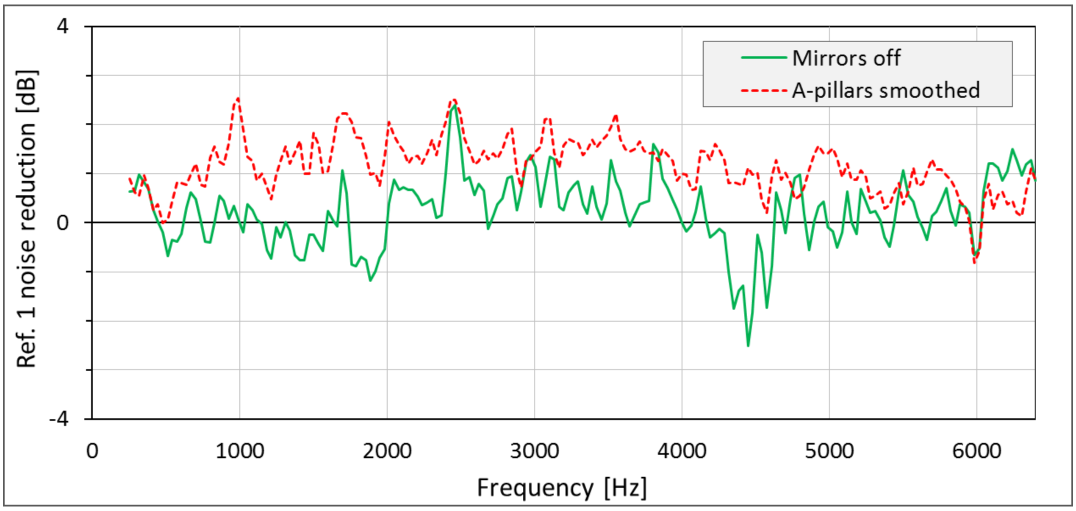

Figure 5 – Reduction in the measured reference 1 auto-power spectrum resulting from taking off the door mirrors and from smoothing the A-pillars.

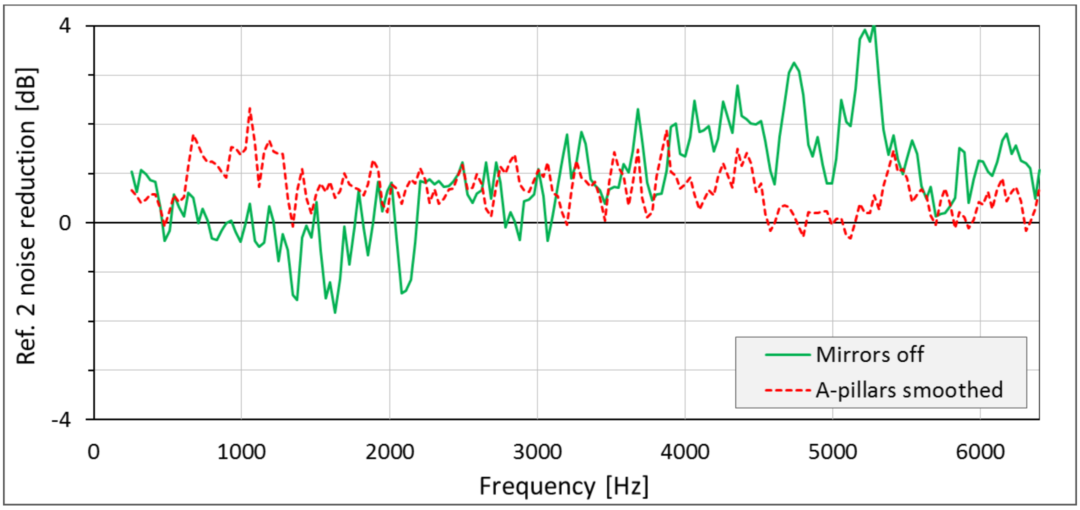

Figure 6 – Reduction in the measured reference 2 auto-power spectrum resulting from taking off the door mirrors and from smoothing the A-pillars.

A set of measurements were performed with the loudspeakers removed, but with wind at a set of different speeds. Only results from measurements with 120 km/h wind speed will be presented here. For the case of loudspeaker sources, all sources except a target source could be easily switched off to measure directly the contribution from the target source. The directly measured target source contribution could then be used for validation of the Clean-SC estimate. For the aerodynamic noise sources around a vehicle, single source contributions cannot be measured directly. Some of the sources can, however, be more or less eliminated without affecting too much other sources. Such a procedure was used for the door mirrors, for the A-pillars and for the front-wheel wells. Only the first two will be considered here. For example for the door mirrors, a measurement was taken with the mirrors in place, and a second measurement was taken with the mirrors removed. The auto-power contribution from the door mirrors to a reference signal could then be estimated as the difference between the auto-power spectrum measured with the mirrors in place and the same spectrum measured with the mirrors removed, but nothing else changed. To estimate the contribution from the A-pillars, measurements were taken with normal A-pillars and with the A-pillars smoothed.

Figure 5 and 6 show the spectral auto-power reductions at reference 1 and reference 2, respectively, obtained by these two modifications. At reference 1, the smoothing of the A-pillars provides a consistent wide-band reduction between 1 and 2 dB, while removal of the mirrors does not produce a clear reduction. At reference 2, the A-pillar smoothing has less effect, but the mirror removal produced reductions up to between 3 and 4 dB in the frequency interval between 3 and 5.5 kHz. In the following, focus will be on reference 2 contributions in the frequency range 3 to 6 kHz.

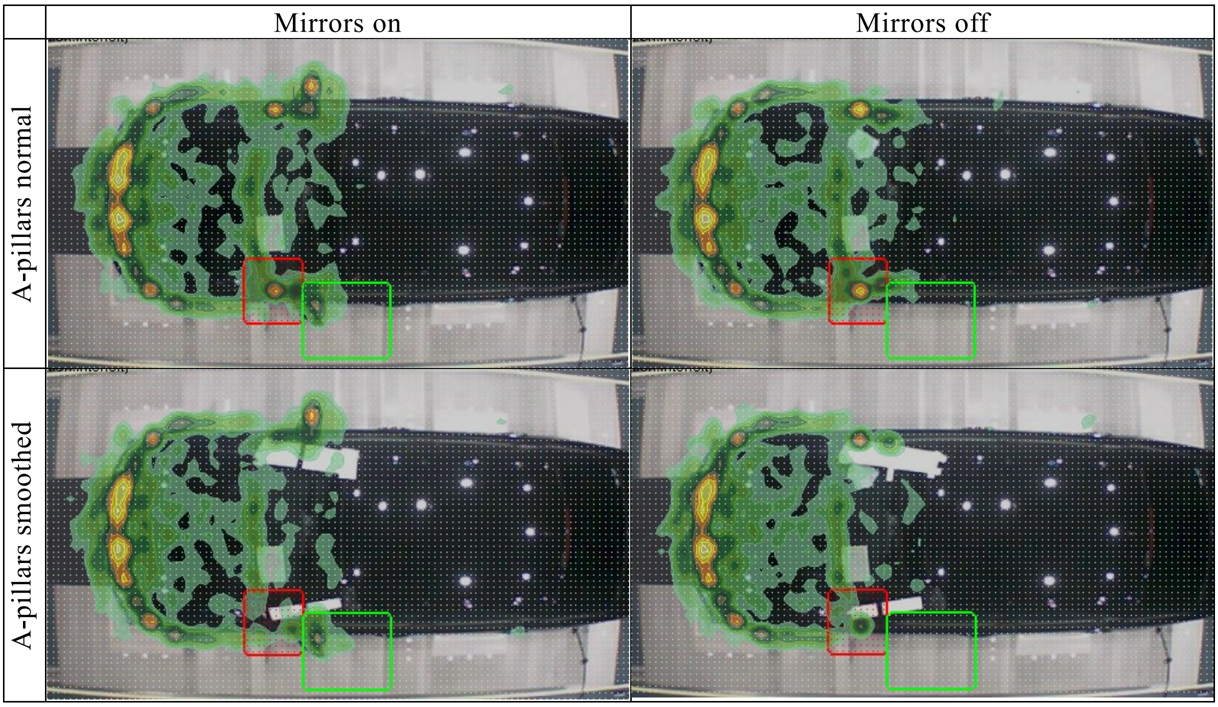

Figure 7 – Contributions to the average array microphone pressure in the frequency range 3 – 6 kHz. All plots use the same color scale with 25 dB display range.

Figure 7 contains results of classical Clean-SC deconvolution, showing contributions to the average sound pressure across the array. The top, left map covers the baseline configuration with the door mirrors in place and without smoothing of the A-pillars. The two modifications are clearly reflected in the other three contour maps: Removal of the door mirrors suppresses the sources sticking out from the car body, and smoothing of the A-pillars reduces the related peaks. With both modifications in place, however, the A-pillar peaks seem to re-appear.

Figure 8 contains contour plots arranged in the same way as those in Figure 7, but showing instead the estimated contributions to reference 2. As expected, the sources on the right side of the car (close to reference 2) have now been emphasized. In particular, the door mirror on that side of the car has a very strong contribution, which agrees with the observation in Figure 6. The contribution to reference

2 from the mirrors can now be estimated by integration over the areas represented by the yellow and green rectangles in the Baseline map at the top left of Figure 8. An evaluation of such an estimate will be described and discussed in the following section.

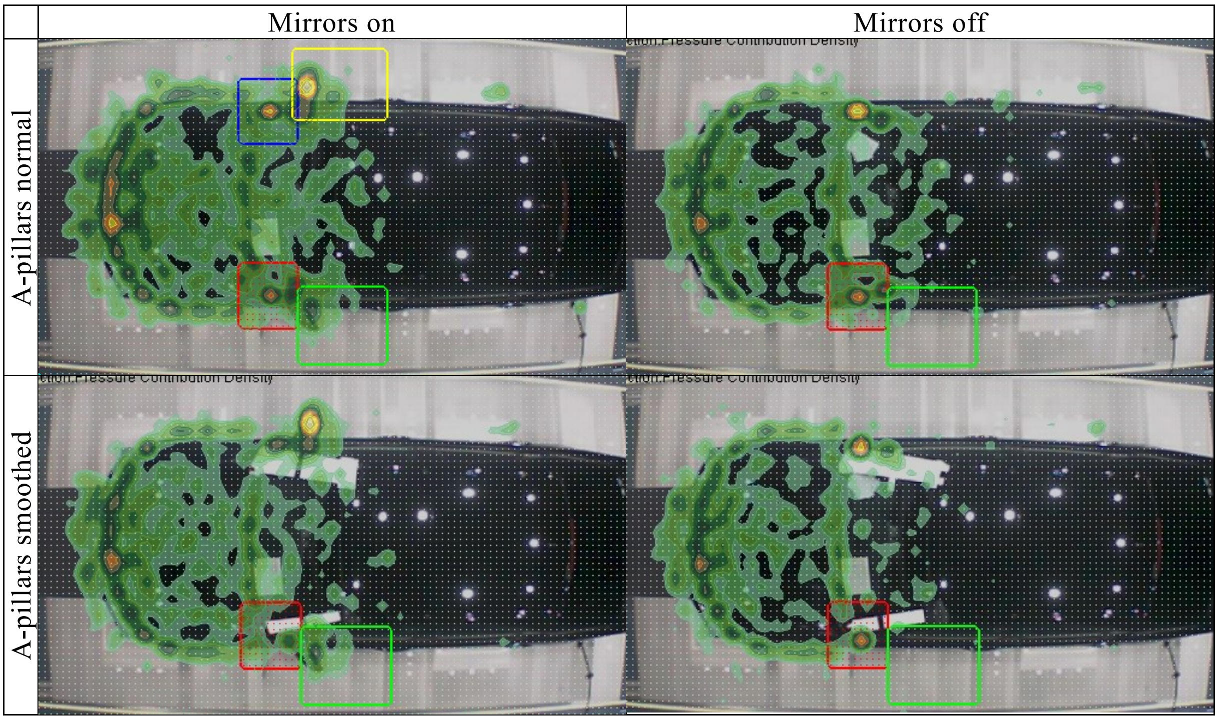

Figure 8 – Ref. 2 contributions in the frequency range 3 – 6 kHz. All plots use the same color scale with 25 dB display range.

3.2.1 **Evaluation of an estimated reference 2 contribution spectrum from the door mirrors**

Area integration over the areas within the yellow and green rectangles in the top left map of Figure 8 will provide an estimate of the contribution at reference 2 from the two door mirrors. An approximate direct measurement of the same contribution can be obtained as the difference between the reference 2 auto-power spectrum with the mirrors in place and a measurement of that spectrum when the two mirrors have been removed. When comparing the two estimates of the contribution, one has to be aware of the following difficulties:

1. Removal of the door mirrors will to some degree influence the noise generation around the A-pillar. As seen in Figure 8, the removal of the mirrors can increase the contribution from the A-pillar.
2. The measured reference microphone spectra before and after removal of the mirrors (see Figure 6) are very close, and both will have some uncertainty, so the difference will be very uncertain. Between 3 and 5.5 kHz, the difference is significant, though, so here a reasonable contribution estimate should be obtained, while below 3 kHz the difference is small and oscillates between positive and negative values.
3. The area-integrated estimates from Clean-SC will be that part of the contribution, which has a significant coherence with the array microphone signals. Incoherent radiation in other directions than the array will not be included.
4. Excitation of the window glass by convecting turbulence will to some degree radiate sound towards the array, but in particular for the top array probably not sufficient to be effectively included. References (5) and (6) investigate the relative importance of window glass excitation from acoustic sources and from turbulence.
5. Coherence loss between the in-cabin reference and the array due to air turbulence will lead to under-estimation.

Figure 9 shows the comparison. The solid black curve represents the increase in reference 2 auto-power introduced by adding the door mirrors. At low frequencies, there are some dropouts, where the measured increase is negative. The red dotted curve, representing the raw output from the Clean-SC area-integration, follows the trend of the solid black curve nicely, but shows a systematic underestimation by 5 to 10 decibel. As can be seen from the above list of difficulties with the comparison, there are many possible reasons for discrepancies. Two obvious reasons for a systematic underestimation are as already mentioned coherence loss due to air turbulence and failure of the array to pick up all independent contributions from the mirrors to the reference signal.

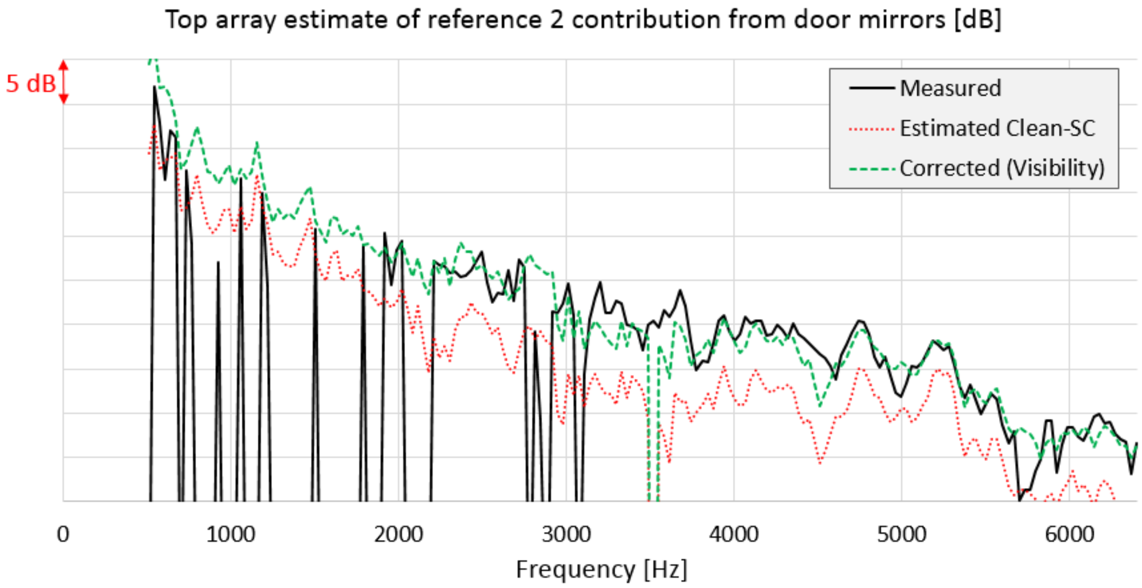

Figure 9 – Spectrum of estimated reference 2 contribution from the door mirrors

The first possible reason, coherence loss, has not yet been thoroughly investigated, but a single measurement with a small narrowband source at 4.6 kHz (a beeper) did not show any sign of significant coherence loss effects. Such effects were not expected either, since earlier investigations on the coherence drop between pairs of array microphones were found to be small in this kind of facility and over the considered frequency range, see reference (7). In the present context, however, a coherence loss between the in-cabin references and the array microphones would be of importance in addition to a coherence loss between pairs of array microphones.

The dashed green curve in Figure 9 was obtained from an attempt to compensate for the array not "seeing" all independent sources introduced by the mirrors: Assume that the fraction of the mirror contributions to reference 2 seen by the top array is equal to the fraction of the full-vehicle contribution to reference 2 seen by the top array. In other words, we assume the underestimation being the same for the mirrors as for the entire vehicle. The full-vehicle contribution is measured directly as the reference 2 auto-power spectrum, and it can be estimated from the Clean-SC contribution map by integration over the full vehicle. The difference between the measured and the estimated full-vehicle contributions is then used to correct the Clean-SC estimate for the mirror contribution, and as a result, we get the dashed green curve in Figure 9. The agreement with the measured mirror contribution is actually very good at the high frequencies, where the difference measurement of the mirror contribution gives a stable result.

One way to include a larger part of the mirror sources in the contribution estimates would be to combine data from the top array and the side array(s). Such an investigation could indicate if the underestimation by Clean-SC in Figure 9 is more or less due to some independent contributions not being picked up by the top array. However, not all directions can be covered, and window glass excitation by convecting turbulence may have too small a contribution at the out-of-flow arrays to be detectable by these.

Even with these limitations, the mapping of contributions to an in-cabin reference instead of contributions at the out-of-flow array will weigh the sources seen by the array according to their contributions at the reference.

4. SUMMARY

A rather simple extension of the Clean-SC algorithm has been presented, capable of mapping the contributions from car-exterior aerodynamic noise sources to a reference signal measured inside the cabin. The algorithm has been validated with very good results through a series of measurements on loudspeakers around a car without wind, and it has been tested with measurements on a car in wind. For the latter case of aerodynamic sources, it is important to be aware that only sources with some minimum contribution at the array will be included in the array results. Acoustic sources radiating in other directions than the array will not be included, and window glass vibration due to convecting turbulence may have a significant contribution in the cabin, but have a too weak contribution at the out-of-flow array. These effects were clearly seen in the results from the wind-tunnel measurements with wind. All results from an out-of-flow array will have these limitations. In the present new application of mapping contributions to an in-cabin reference they just became visible. The mapping of contributions to an in-cabin reference instead of contributions at the out-of-flow array, however, has the advantage of weighing the sources seen by the array according to their contributions at the in-cabin reference.

REFERENCES

1. Ehrenfried, K. and Koop, L. A comparison of iterative deconvolution algorithms for the mapping of acoustic sources. Proc 12th AIAA/CEAS Aeroacoustics Conference (27th AIAA Aeroacoustics Conference); 2006; Paper no. AIAA 2006-2711.
2. Sijtsma P. CLEAN Based on Spatial Source Coherence. Proc 13th AIAA/CEAS Aeroacoustics Conference (28th AIAA Aeroacoustics Conference); 2007; Paper no. AIAA 2007-3436.
3. Hald J. Cross-spectral matrix diagonal reconstruction. Proc INTER-NOISE 16; 21-24 August 2016; Hamburg; Germany 2016.
4. Bendat S.B. and Piersol A.G. Engineering Applications of Correlation and Spectral Analysis. John Wiley & Sons; 1980.
5. Bremner P.G. Vibroacoustic Source Mechanisms under Aeroacoustic Loads. Proc 18th AIAA/CEAS Aeroacoustics Conference (33rd AIAA Aeroacoustics Conference); 4-6 June 2012; Paper no. AIAA 2012-2206.
6. Hartmann M. et. al. Wind Noise caused by the A-pillar and the Side Mirror flow of a Generic Vehicle Model. Proc 18th AIAA/CEAS Aeroacoustics Conference (33rd AIAA Aeroacoustics Conference); 4-6 June 2012; Paper no. AIAA 2012-2205.
7. Dougherty R.P. Turbulent Decorrelation of Aeroacoustic Phased Arrays: Lessons from Atmospheric Science and Astronomy. Proc 9th AIAA/CEAS Aeroacoustics Conference and Exhibit; 12-14 May 2003; Paper no. AIAA 2003-3200.